



## Theoretical model to determine the Porosity and refractive index of porous silicon type-n by using Atomic force microscope

**Wasna'a M. Abdulridha<sup>1</sup>, Ahmed N. Abd<sup>2,\*</sup>, Mohammed O. Dawood<sup>2</sup>**

<sup>1</sup>Basic Science Department, University of Al- Kufa, Najaf, Iraq

<sup>2</sup>Physics Department, Science Faculty, University of Al- Mustansiriyah, Baghdad, Iraq

\*E-mail address: [ahmed\\_naji\\_abd@yahoo.com](mailto:ahmed_naji_abd@yahoo.com)

### ABSTRACT

Porous silicon (PS) layer was produced by photochemical etching process at (5, 7, 10, 12 and 15) etching time and  $7 \text{ mA/cm}^2$  current density then after investigation by Atomic Force Microscope (AFM) the thickness of PS layer from about  $3.4 \mu\text{m}$  to  $15.8 \mu\text{m}$  was determined. The surface of porous silicon is formed from small pyramids with porous structure, where the porosity of n-PS is from  $\approx$  (32-72%). Porous silicon layer formed on the silicon substrates by photochemical etching contains also the nanopores with diameter about (16.41-42) nm in current density ( $7\text{mA/cm}^2$ ). The porosity and thickness was determined from AFM results and compared with the result from the usually measured porosity and thickness through a gravimetric method we found that the values of porosity and thickness calculated from two methods are approximately similar to each other with few difference, the influence of structure changes on optical properties such as refractive index, which decreases exponentially with porosity.

**Keywords:** Porous Silicon; refractive index; porosity; thickness and AFM

## 1. INTRODUCTION

The atomic force microscope (AFM) or scanning force microscope (SFM) was invented in 1986 by Binnig, Quate and Gerber. Similar to other scanning probe microscopes, the AFM raster scans a sharp probe over the surface of a sample and measures the changes in force between the probe tip and the sample. Figure (1) illustrates the working concept for an atomic force microscope [1].

A cantilever with a sharp tip is positioned above a surface. Depending on this separation distance, long range or short range forces will dominate the interaction. This force is measured by the bending of the cantilever by an optical lever technique: a laser beam is focused on the back of a cantilever and reflected into a photodetector. Small forces between the tip and sample will cause less deflection than large forces. By raster-scanning the tip across the surface and recording the change in force as a function of position, a map of surface topography and other properties can be generated [2,3].

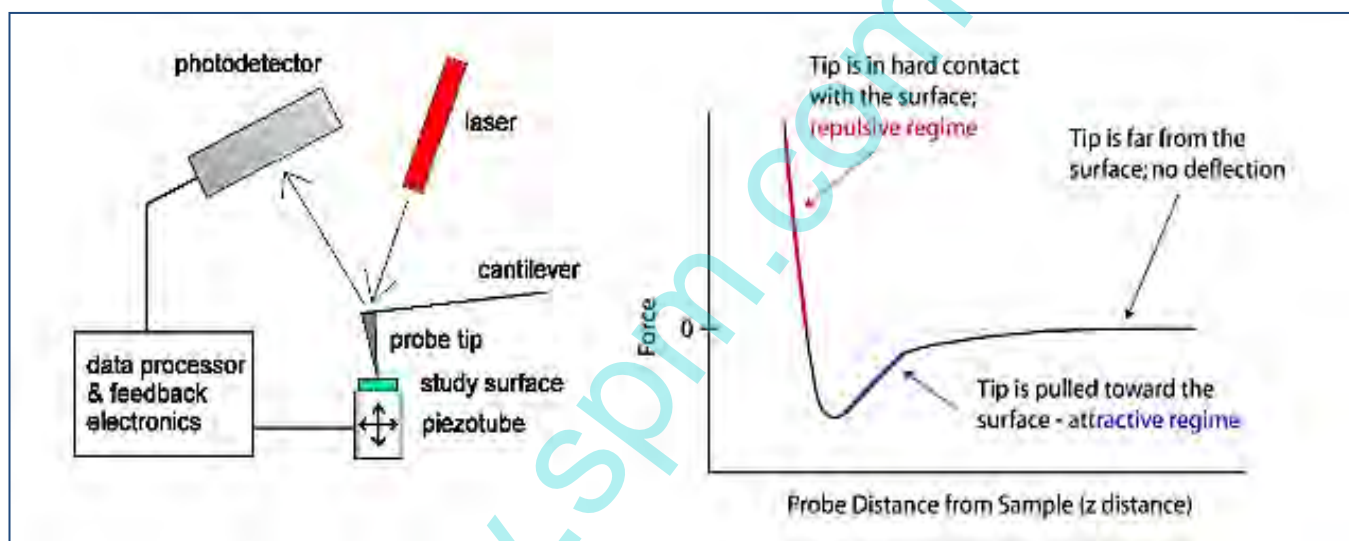


Fig. 1. Scheme of an atomic force microscope and the force-distance curve characteristic of the interaction between the tip and sample [2].

The AFM is useful for obtaining three-dimensional (3D) topographic information of insulating and conducting structures with lateral resolution down to 1.5 nm and vertical resolution down to 0.05nm [4]. These samples include clusters of atoms and molecules, individual macromolecules, and biological species (cells, DNA, proteins). Unlike the preparation of samples for STM imaging, there is minimal sample preparation involved for AFM imaging [5].

Similar to STM operation, the AFM can operate in gas, ambient, and fluid environments and can measure physical properties including elasticity, adhesion, hardness, friction and chemical functionality.

## 2. EXPERIMENTAL WORK

Porous silicon wafers were cut into  $(1.5 \times 1.5) \text{ cm}^2$  compatible with the dimension of substrate holder by using a steel cutter tool.

The Si samples were cleaned with alcohol and an ultrasonic bath in order to remove the impurities and residuals from their surface. These substrates were etched with HF (10%) for 5 min to remove the native oxide. Thin homogenous PSi layer of various thicknesses were formed on the frontal surface of the material using photoelectrochemical etching process (PEC).

Photochemical anodization was performed under illumination to produce porous Si layers on polished n-type, (100) oriented Si wafers with a resistivity of  $(1-4.5) \Omega \cdot \text{cm}$  and a thickness of  $\approx 500 \mu\text{m}$ , using a 1:1 mixture of 40 % HF: 99.99 % ethanol as an electrolyte.

Initially, the Si wafers were cleaned successively by ethyl alcohol and deionized water. Thick Al films,  $\approx 1 \mu\text{m}$  thick, were rf-sputter-deposited on the back side of the wafers and then annealed at  $350 \text{ }^\circ\text{C}$  for 2 hour in vacuum to form good ohm contacts (because of the formation of a  $n^-$  layer).

The anodization was carried out with the distance between the Si substrate to the Au counter electrode fixed at  $\approx 1.5 \text{ cm}$ , using a current density of  $(7 \text{ mA/cm}^2)$  for a variation etching times of (5,7,10,12 and 15) min as shown in Figure (2).

After the anodization, the PS layers were dried in the following way to reduce the capillary stress using pentane, which has very low surface tension and no chemical reactivity with the PS layer.

The samples were rinsed first with gold, then with 99.99 % methanol and finally with deionized water. ext, the samples were dried at about  $30 \text{ }^\circ\text{C}$ , the surface profiles were analyzed by atomic force microscopy or AFM (Topometrix-Accurex II).

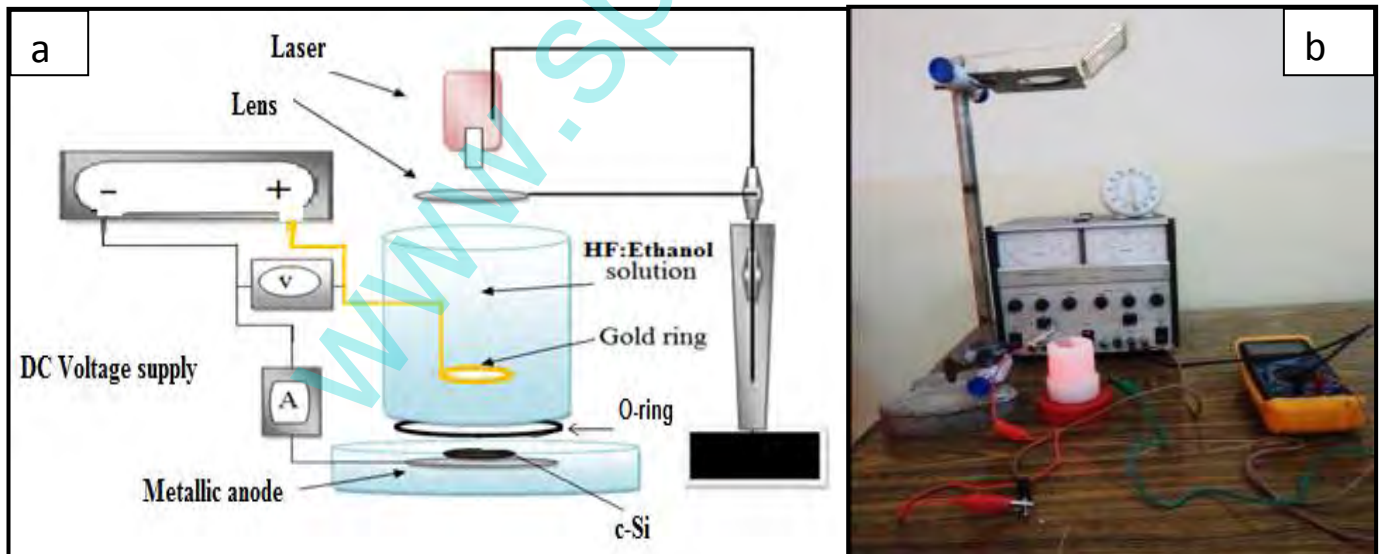


Fig. 2a. The schematic diagram of PEC system, b) The photographic image of PEC system.

### 3. THEORETICAL MODEL

PS porosity “P” is defined as the fraction of void within the PS layer and can be determined easily by weight measurements. The virgin wafer is first weighed before anodisation (m1), then just after The higher current causes more solving silicon and anodisation (m2) and finally after dissolution of the whole porous layer in a molar KOH aqueous solution (m3):

$$p (m)\% = \frac{m1 - m3}{m1 - m2} \dots \dots \dots (1)$$

The removal is made through a dip for some minutes in an aqueous solution of KOH (3% in volume), that leads to a selective removal of the PS layer without reacting with the bulk crystalline silicon. Different techniques are employed to determine the porous layer thickness d. From the gravimetric measurements:

$$d = \frac{m1 - m3}{\rho S} \dots \dots \dots (2)$$

where ρ is the silicon density and S the etched surface area, thickness of PS layer tunable to the depth of the hole left after dissolution of the PS layer [5]. This method destroys the sample and KOH cause to remove the aluminum layer that deposited on the back face of Si wafer which cause to variation in the value of (m3), so we found nondestructive method depending on AFM measurement. We calculate the porosity and thickness by AFM technique with five steps:

- (1) Since the AFM can measure the pore diameter and depth and also can measure mean roughness and mean number of pores in given length, we can calculate the pore volume and total volumes of all pores in etched area for all samples.
- (2) We consider the pore shape as cone, so its volume (v) (in all etched area is: (n/3) πr<sup>2</sup>h; where: r is pore radius, h is pore depth, and n is number of pores in etched area.
- (3) We calculate the weight of removed part of silicon from the following relation:

$$v \cdot \rho = m1 - m2 \dots \dots \dots (3)$$

where ρ the silicon density and equals to 2.33 g/cm<sup>3</sup>

- (4) AFM can measure film thickness d (nm), so we can calculate m1 – m3 from the following relation:

$$m1 - m3 = d \cdot \rho \cdot s - v \cdot \rho \dots \dots \dots (4)$$

- (5) The porosity p (m)% in this method by Eq. (1).
- (6) Determination of Refractive Index From the optical transmittance (T) of PS film. Refractive index n<sub>s</sub> of different PS films can be calculated as follows [6]:
- (7) The necessary values of the refractive index of the substrate n<sub>s</sub>, are obtained from the transmission spectrum of the substrate (T) using the well-known [7,8]:

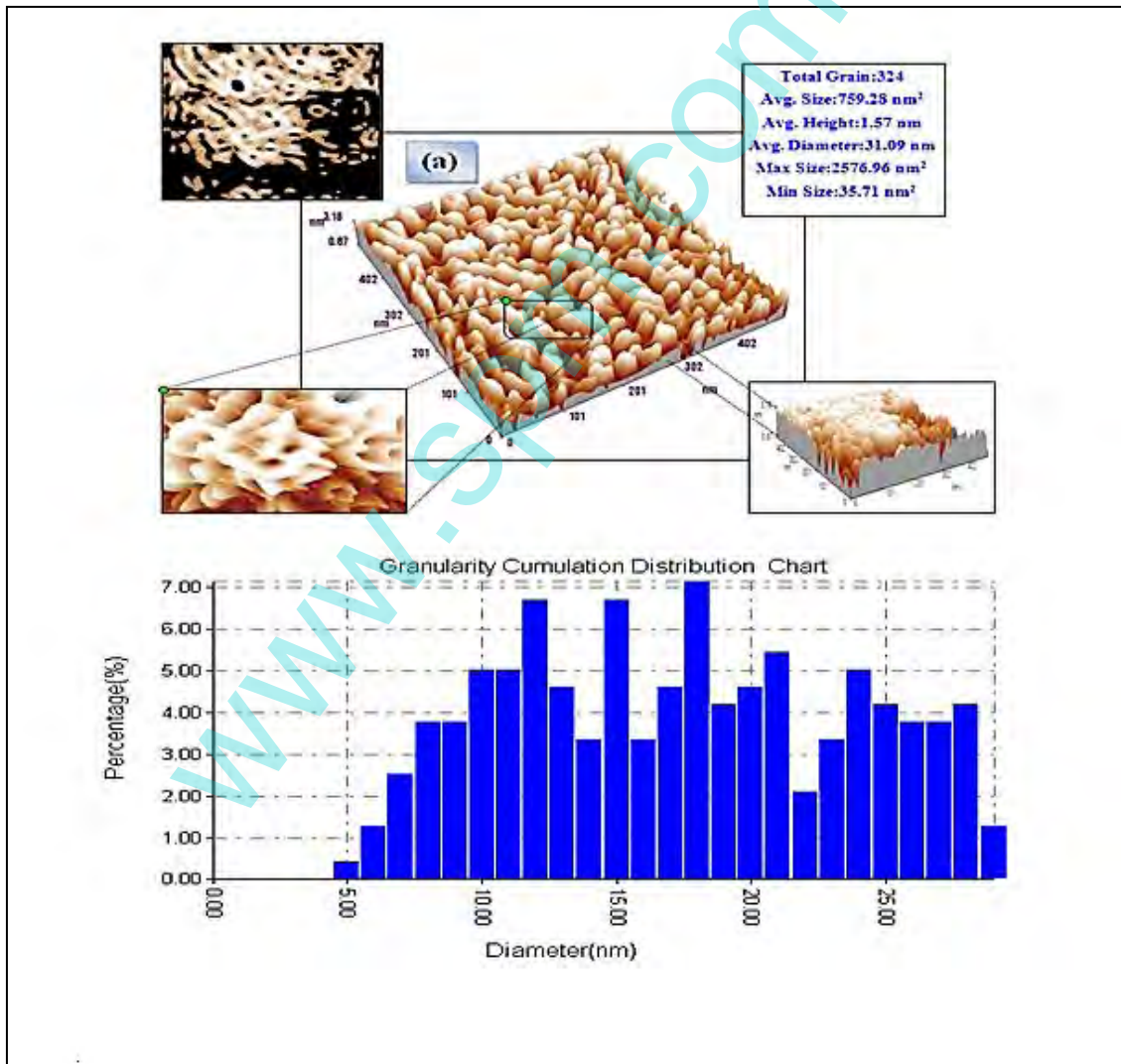
$$n_s = T^{-1} + (T^{-1}-1)^{0.5} \dots\dots\dots (5)$$

(8) In term of Eq. (6), refractive index of the film  $n_1$  in the spectral region of weak absorption ( $\approx 0$ ) can be calculated:

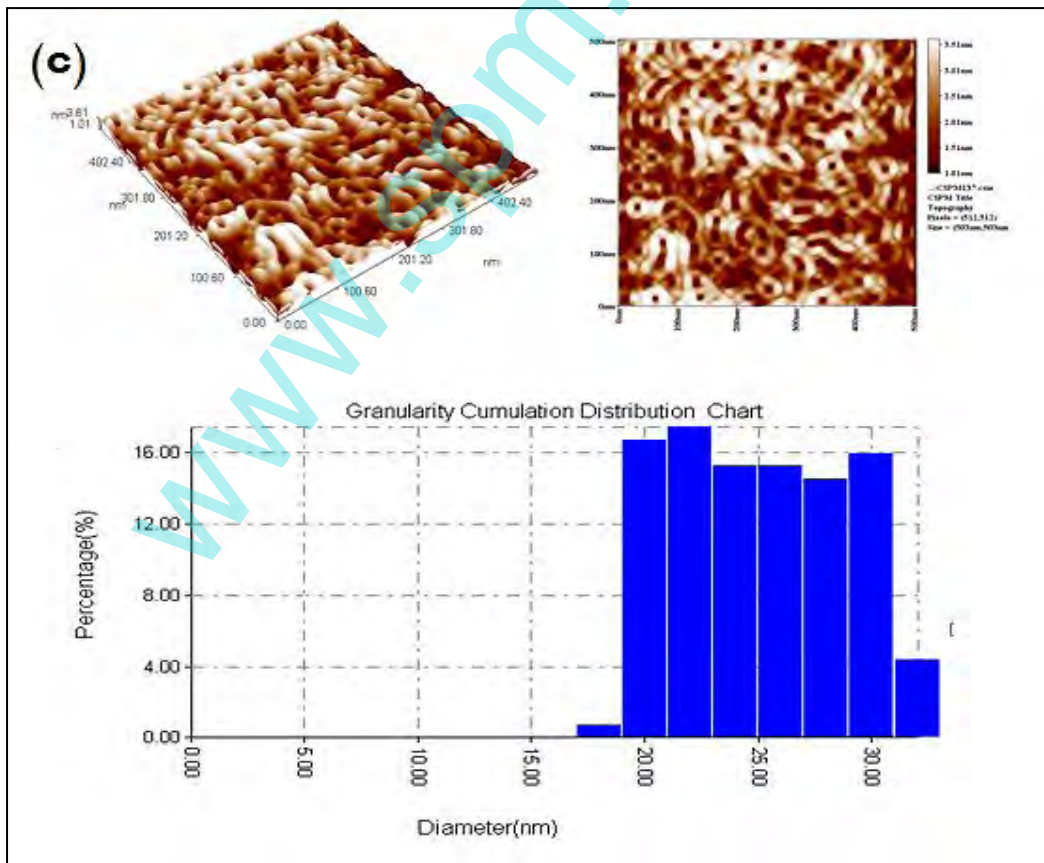
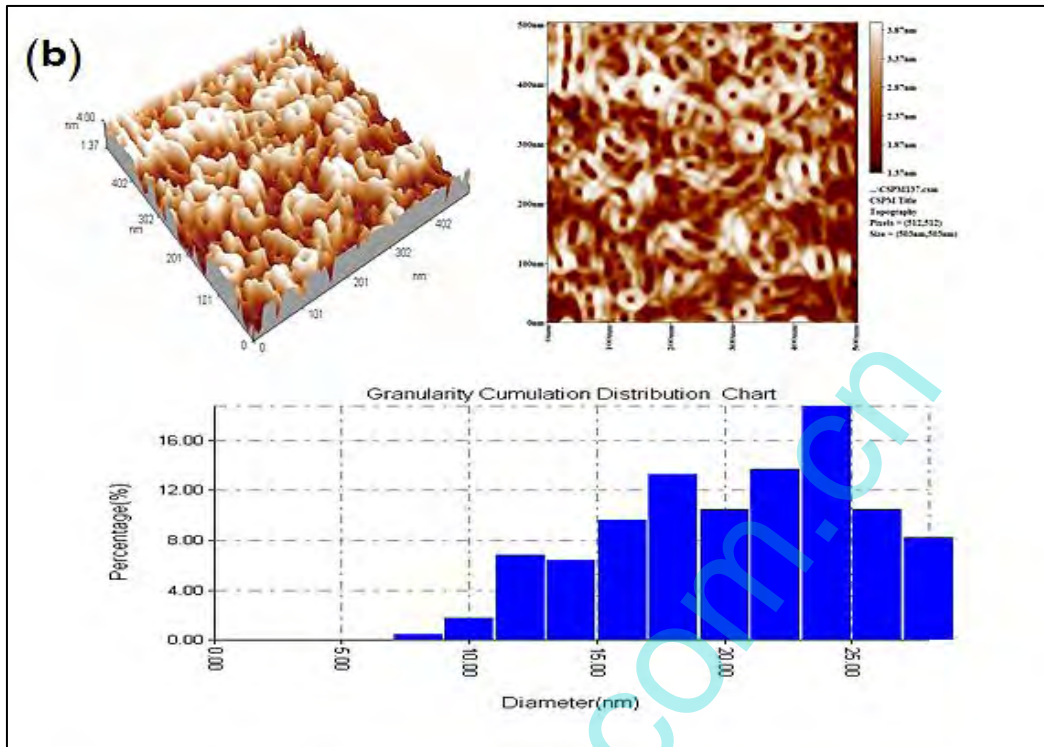
$$n_1 = \sqrt{n_s} \frac{\sqrt{(1+\sqrt{R})}}{\sqrt{(1-\sqrt{R})}} \dots\dots\dots (6)$$

#### 4. RESULTS AND DISCUSSION

Figure (3a,b,c,d and e) show five examples as 3D images of porous silicon prepared at different etching times with fixed etching current density, it allow us to calculate average diameter, depth, porosity and thickness by applied equations (1,3 and 4).Also, show a better distribution and porosity at 15 min etching time as shown in Figures (3 ) respectively.







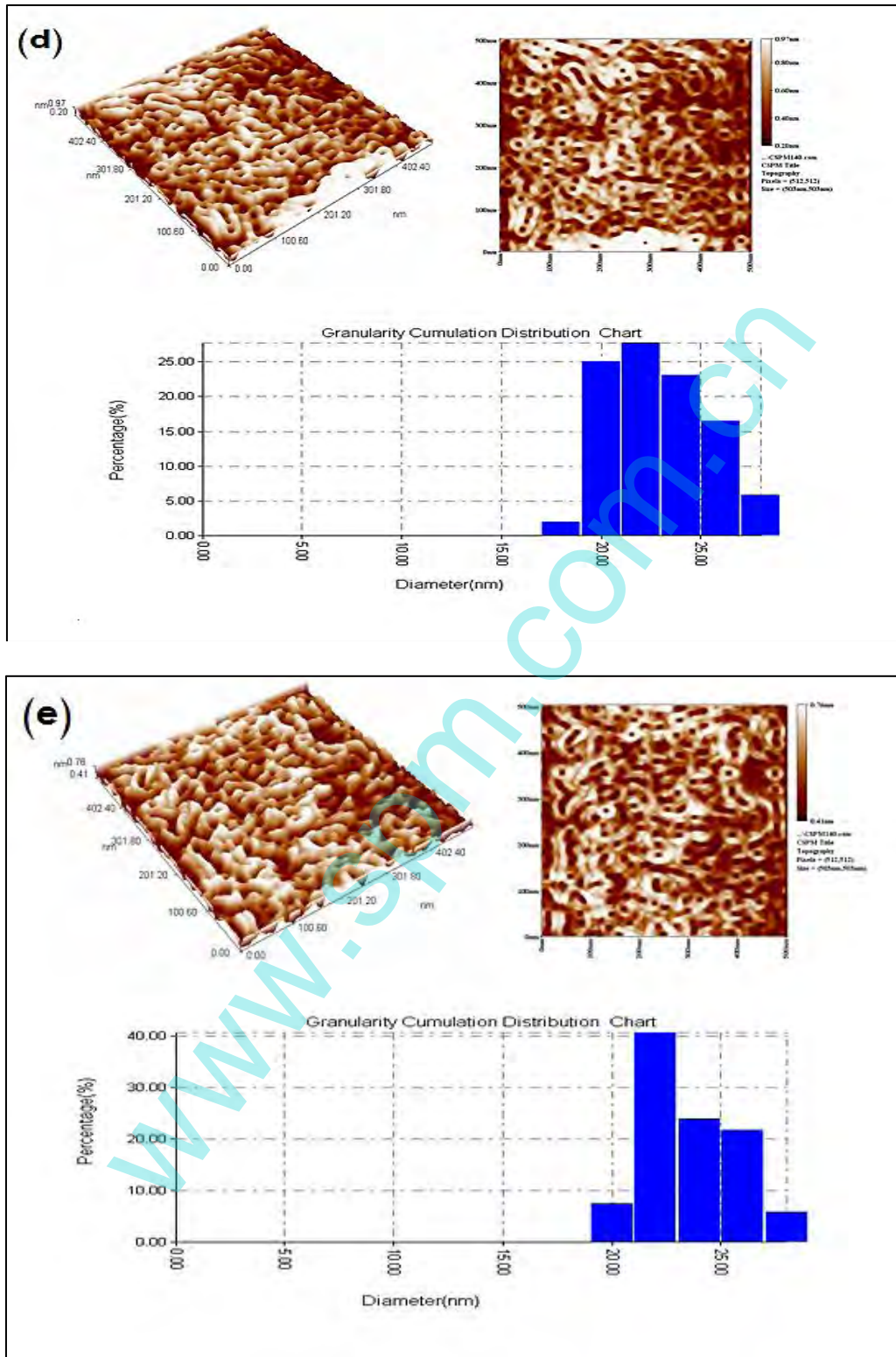


Fig. 3. 3D, 2D AFM images ( $0.5 \mu\text{m}^2 \times 0.5 \mu\text{m}^2$ ) and Granularity accumulation distribution chart of porous silicon samples prepared with etching time of (5,7,10,12 and 15) min at current density of  $7 \text{ mA/cm}^2$ .

Also, the surface of porous silicon is formed from small pyramids with porous structure, Figure (4) shows the comparison between the values of porosity of n-PS that calculated from AFM and gravimetric method, the values of porosity approximately are similar, and ranging from  $\approx$  (32-72%)

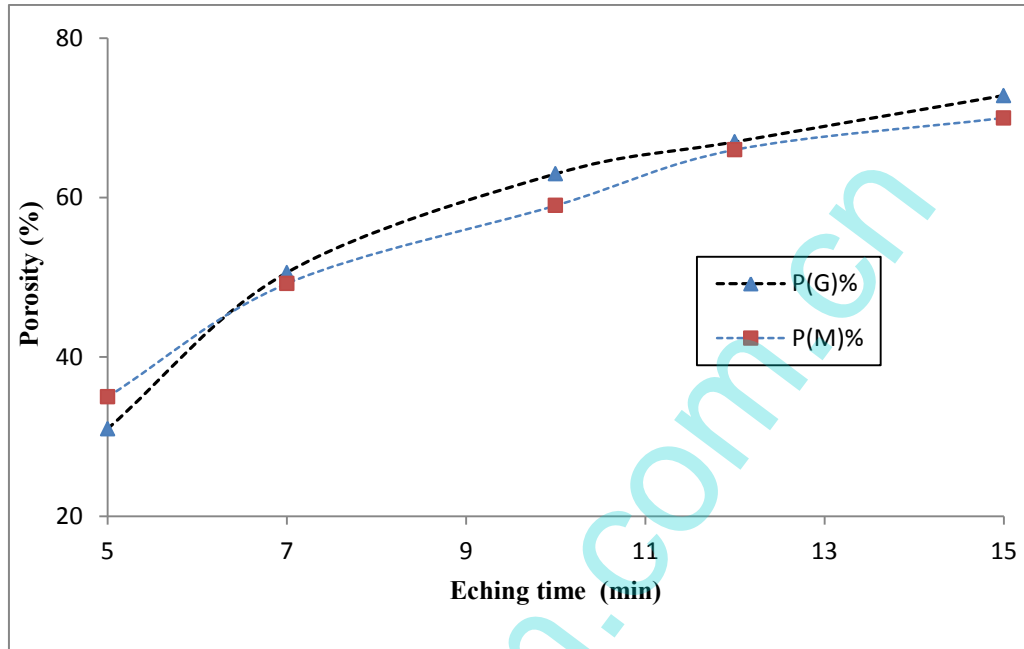


Fig. 4. Porosity calculated from AFM and measured from gravimetric method.

The PS layer thickness is in related to etching time, i.e. increasing the thickness of PS layer is attributed to increase etching times because of increasing pore width with arrived enough no of holes to the wafer surface, so that PS layer thickness represent an important parameter and can be calculated from AFM and gravimetric (G) methods as illustrated in Table (1), which exhibits the variation in thickness values that obtained from these methods.

Table 1. Porosity and thickness calculated from both AFM and gravimetric method.

| Etching times (min) | Porosity % |    | Thickness ( $\mu\text{m}$ ) |       |
|---------------------|------------|----|-----------------------------|-------|
|                     | AFM        | G  | AFM                         | G     |
| 5                   | 36         | 30 | 3.4                         | 3.1   |
| 7                   | 48         | 51 | 3.7                         | 3.96  |
| 10                  | 59         | 62 | 6.4                         | 7.1   |
| 12                  | 62.5       | 63 | 11.5                        | 12.13 |
| 15                  | 68         | 71 | 15.8                        | 16.7  |



Figure (5) shows the comparison between the values of PS layer thickness of n-PS that calculated from each method, the values of thickness approximately are similar, and ranging from  $\approx (3.1-16.7) \mu\text{m}$ .

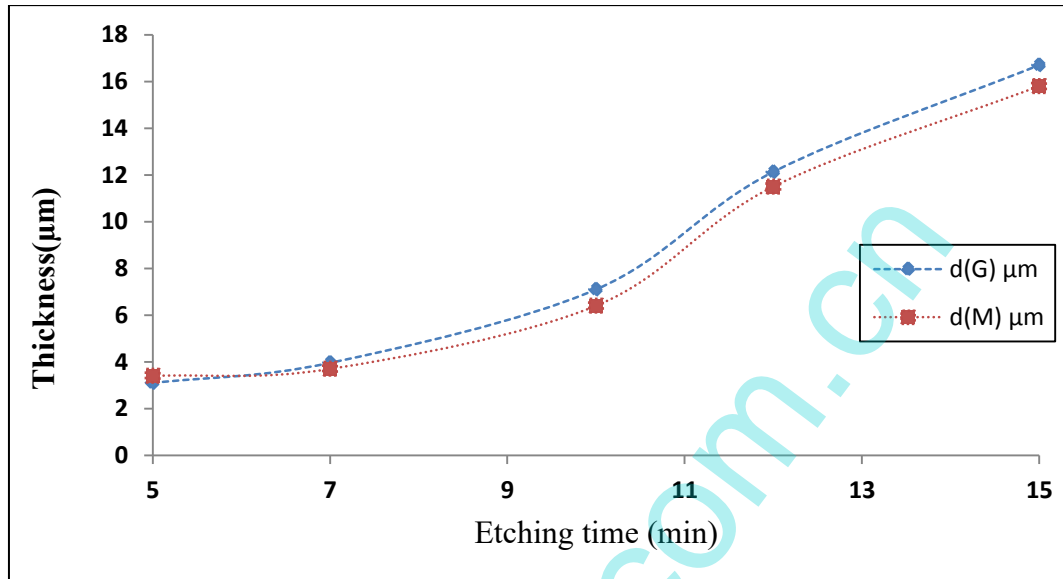


Fig. 5. Thickness of PS layer calculated from AFM and gravimetric method.

By using special software (Imager 4.62, CSPM System Palette), the estimated values of root mean square RMS of surface roughness average and average grain size were calculated and listed in Table (2). The porous fabricated with  $(7 \text{ mA/cm}^2)$  current density and 5 min etching time have average diameter (16.41 nm) as shown in Figure (2a) and the surface is very smooth while the sample that prepared at 15min etching time exhibit high rough surface and this attributed to increasing the porosity.

The grain size and the root mean square of surface roughness increases when etching time increases. 3D images prove that the grains are uniformly distributed within the scanning area (500 nm x500 nm) with individual columnar pore extending upwards. This surface characteristic is important in photodetector (PD).

**Table 2.** The Average diameter, roughness average and Root mean square of of porous silicon samples prepared with etching time of (5,7,10,12 and 15) min at current density of  $7 \text{ mA/cm}^2$ .

| Etching time (min) | Average Grain size (nm) | Roughness average (nm) | Root mean square (nm) |
|--------------------|-------------------------|------------------------|-----------------------|
| 5                  | 16.41                   | 0.644                  | 0.557                 |
| 7                  | 18.4                    | 0.610                  | 0.708                 |
| 10                 | 22.7                    | 0.602                  | 0.701                 |

|    |      |       |        |
|----|------|-------|--------|
| 12 | 23.2 | 0.177 | 0.206  |
| 15 | 42.0 | 0.795 | 0.0924 |

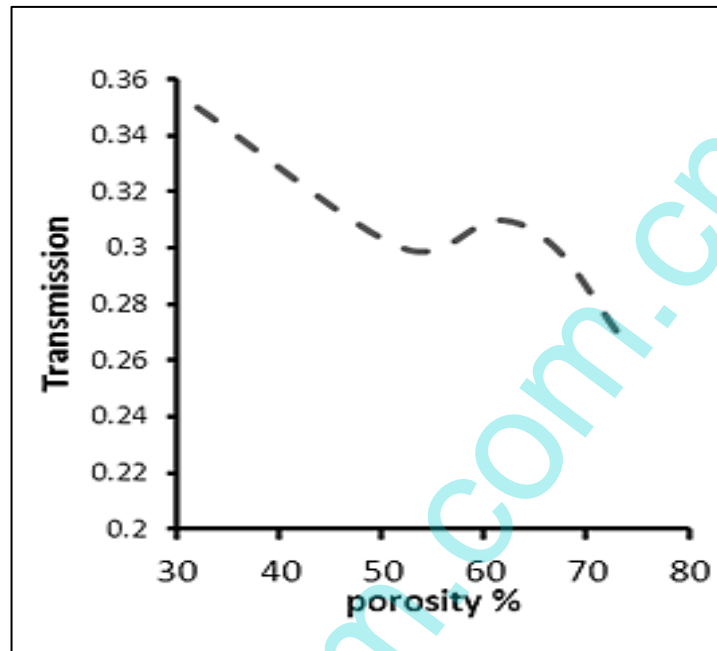


Fig. 6. Transmission as function of porosity for n-type.

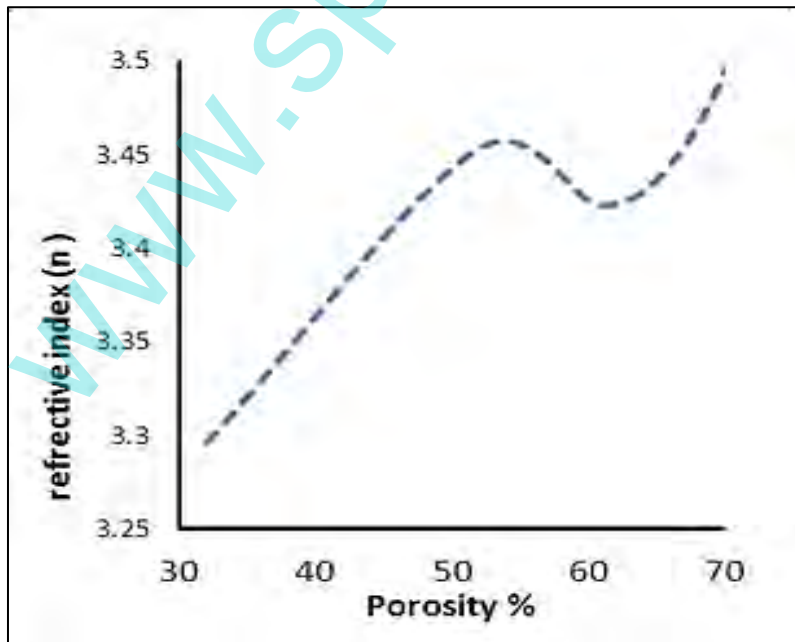


Fig. 7. Refractive index as function of porosity for n-type.

The porous fabricated with ( $7 \text{ mA/cm}^2$ ) current density and 15 min etching time have average diameter (42 nm) as shown in Figure (2e). From optical transmittance of PS, the refractive index of the substrate and PS layer was determined by using the equation (5 and 6). All the results found to be agree with the theoretical parameters.

It was observed that with increased membrane porosity, the transmitted light intensity decreases and the refractive index increases as shown in Figure 6 and 7 respectively. The membranes had poor transparency at shorter wavelengths ( $k < 600 \text{ nm}$ ) because of the fundamental optical absorption in Si. The calculated refractive indices ( $k > 600 \text{ nm}$ ) of PS films were in qualitative agreement with those expected by the effective medium theory (i.e. a higher porosity results in higher index of refraction).

#### 4. CONCLUSIONS

Samples of porous silicon (PS) were prepared by photochemical etching process, their structures were studied with AFM, the AFM results were used to calculate the porosity and thickness in addition to gravimetric technique. The AFM technique is the best as compare with gravimetric method because it doesn't destroy the samples, and it is the best in case of deposited thick aluminum layer on the back face of silicon wafer to achieve high stability of current distribution.

#### Reference

- [1] R.J. Žvalionienė, V. Grigaliūnas, S. Tamulevičius, "Fabrication of porous silicon microstructures using electrochemical etching", *Materials Science (Medžiagotyra)* 9(4) (2003) 1392-1320.
- [2] S.H. Mohameda, E.R. Shaabanb, "Investigation of the refractive index and dispersion parameters of tungsten ox nitride thin films", *Materials chemistry and Physics* 121 (2010) 249-253.
- [3] Park J.H., Gu L., von Maltzahn G., Ruoslahti E., Bhatia S.N., Sailor M.J., Biodegradable luminescent porous silicon nanoparticles for in vivo applications. *Nat. Mater.*, 8 (2009) 331-336.
- [4] Ferrari, M. Cancer nanotechnology: opportunities and challenges. *Nat. Rev. Cancer*, 5 (2005) 161-171.
- [5] Bharali D.J., Khalil M., Gurbuz M., Simone T.M., Mousa A.S., Nanoparticles and cancer therapy: A concise review with emphasis on dendrimers. *Int. J. Nanomed*, 4 (2009) 1-7.
- [6] Popp U., Herbig R., Michel G., Müller E., Oestreich C., Properties of Nanocrystalline Ceramic Powders Prepared by Laser Evaporation and Recondensation. *J. Eur. Ceram. Soc.*, 18 (1998) 1153-1160.
- [7] H.S. Tamboli, V. Puri, R.K. Puri, R.B. Patil, M.F. Luo, Comparative study of physical properties of vapor chopped and nonchopped  $\text{Al}_2\text{O}_3$  thin films, *Materials Research Bulletin* 46 (2011) 815-819.

- [8] Kelly, P.J.; Arnell, R.D., Magnetron sputtering: a review of recent developments and applications. *Vacuum*, 56 (2000) 159-172.

( Received 16 October 2015; accepted 02 November 2015 )

[www.spm.com.cn](http://www.spm.com.cn)